

# Cellular Mechanisms for Dopamine D<sub>4</sub> Receptor-induced Homeostatic Regulation of $\alpha$ -Amino-3-hydroxy-5-methyl-4-isoxazolepropionic Acid (AMPA) Receptors<sup>\*[5]</sup>

Received for publication, January 13, 2011, and in revised form, May 25, 2011. Published, JBC Papers in Press, May 27, 2011, DOI 10.1074/jbc.M111.221416

Eunice Y. Yuen and Zhen Yan<sup>1</sup>

From the Department of Physiology and Biophysics, School of Medicine and Biomedical Sciences, The State University of New York at Buffalo, Buffalo, New York 14214

Aberrant dopamine D<sub>4</sub> receptor function has been implicated in mental illnesses, including schizophrenia and attention deficit-hyperactivity disorder. Recently we have found that D<sub>4</sub> receptor exerts an activity-dependent bi-directional regulation of AMPA receptor (AMPA) receptor (AMPA)-mediated synaptic currents in pyramidal neurons of prefrontal cortex (PFC) via the dual control of calcium/calmodulin kinase II (CaMKII) activity. In this study, we examined the signaling mechanisms downstream of CaMKII that govern the complex effects of D<sub>4</sub> on glutamatergic transmission. We found that in PFC neurons at high activity state, D<sub>4</sub> suppresses AMPAR responses by disrupting the kinesin motor-based transport of GluR2 along microtubules, which was accompanied by the D<sub>4</sub> reduction of microtubule stability via a mechanism dependent on CaMKII inhibition. On the other hand, in PFC neurons at the low activity state, D<sub>4</sub> potentiates AMPAR responses by facilitating synaptic targeting of GluR1 through the scaffold protein SAP97 via a mechanism dependent on CaMKII stimulation. Taken together, these results have identified distinct signaling mechanisms underlying the homeostatic regulation of glutamatergic transmission by D<sub>4</sub> receptors, which may be important for cognitive and emotional processes in which dopamine is involved.

The mesocortical dopamine inputs from ventral tegmental area to prefrontal cortex (PFC)<sup>2</sup> is involved in many cognitive functions, such as motivation (1), reinforcement learning (2), and working memory (3, 4). Dopamine exerts its action via D<sub>1</sub>-like (D<sub>1</sub>, D<sub>5</sub>) and D<sub>2</sub>-like (D<sub>2</sub>, D<sub>3</sub>, D<sub>4</sub>) receptors (4, 5). D<sub>4</sub> receptor (D<sub>4</sub>R) is preferentially distributed in PFC (6, 7), suggesting its prominent role in this brain area.

D<sub>4</sub> receptor is of particular interest because of its potent affinity to atypical antipsychotics, such as clozapine, which has fewer extrapyramidal side effects compared with typical antipsychotics with D<sub>2</sub> antagonism (8, 9). The D<sub>4</sub>R gene polymor-

phisms with variable tandem repeats have been implicated in the prevalence of several mental disorders, including attention deficit-hyperactivity disorder (ADHD) (10, 11), Tourette syndrome (12), and substance abuse (13, 14). Moreover, human studies suggest that the gene polymorphisms correlate with the PFC gray matter volume (15) and responsiveness to medication in ADHD patients (16). In animal studies, mice lacking D<sub>4</sub>R show cortical hyperexcitability (17), decreased novelty exploration (18), and increased locomotor sensitivity to psychostimulants (19). These findings support the essential role of D<sub>4</sub>R in normal PFC functioning as well as in many neuropsychiatric disorders.

Growing evidence suggests a homeostatic function of D<sub>4</sub> receptors in PFC. Behavioral studies show that a D<sub>4</sub> antagonist may enhance or suppress working memory depending on the base-line performance (20). Our previous studies have identified two homeostatic targets of D<sub>4</sub>: CaMKII and AMPAR (21, 22). At high neuronal activity, D<sub>4</sub> suppresses AMPAR-mediated synaptic transmission by decreasing CaMKII activity. Conversely, at low neuronal activity, D<sub>4</sub> potentiates AMPAR trafficking and function by increasing CaMKII enzymatic activity and synaptic redistribution (22, 23). Such a D<sub>4</sub>-mediated, state-dependent homeostatic mechanism could be highly relevant to the pathophysiology of ADHD and schizophrenia, in which weakened D<sub>4</sub> function and dysregulation of glutamatergic transmission have been implicated. In this study, we have dissected out the mechanisms downstream of CaMKII that are responsible for the activity-dependent bi-directional regulation of AMPARs by D<sub>4</sub> in PFC pyramidal neurons.

## MATERIALS AND METHODS

**Synaptic Current Recording in PFC Cultures**—All experiments were carried out with the approval of the State University of New York at Buffalo Animal Care Committee. PFC cultures were prepared from 18-day rat embryos and maintained for 3–4 weeks *in vitro*. In some experiments, cultures were pretreated with the GABA<sub>A</sub> receptor antagonist bicuculline (10  $\mu$ M, 2 h) or TTX (0.5  $\mu$ M, 2 h) to elevate or dampen basal neuronal activity, respectively. AMPAR-mediated mEPSC was recorded as described previously (24). The internal solution contained 130 mM cesium methanesulfonate, 10 mM CsCl, 4 mM NaCl, 1 mM MgCl<sub>2</sub>, 10 mM HEPES, 5 mM EGTA, 2.2 mM lidocaine, 12 mM phosphocreatine, 5 mM MgATP, 0.5 mM Na<sub>2</sub>GTP, 0.1 mM leupeptin, pH 7.2–7.3, 265–270 mOsm. The external solution contained 127 mM NaCl, 5 mM KCl, 2 mM MgCl<sub>2</sub>, 2 mM CaCl<sub>2</sub>, 12

\* This work was supported, in whole or in part, by National Institutes of Health Grant MH84233 (to Z. Y.).

[5] The on-line version of this article (available at <http://www.jbc.org>) contains supplemental Fig. 1.

<sup>1</sup> To whom correspondence should be addressed: Dept. of Physiology and Biophysics, State University of New York at Buffalo, 124 Sherman Hall, Buffalo, NY 14214. E-mail: zhenyan@buffalo.edu.

<sup>2</sup> The abbreviations used are: PFC, prefrontal cortex; ADHD, attention deficit-hyperactivity disorder; CaMKII, calcium/calmodulin kinase II; mEPSC, miniature excitatory postsynaptic current; R, receptor; SAP97, synapse-associated protein 97; TTX, tetrodotoxin; MT, microtubule.

## Mechanisms for $D_4$ Modulation of AMPARs

mM glucose, 10 mM HEPES, 0.0005 mM TTX, pH 7.3–7.4, 300–305 mOsm. The membrane potential was held at  $-70$  mV. Synaptic currents were analyzed with Mini Analysis Program (Synaptosoft, Leonia, NJ). Statistical comparisons of the amplitude and frequency of mEPSC were made using the Kolmogorov-Smirnov test.

Dopamine  $D_4$  receptor agonist PD168077 maleate and the cytoskeleton disturbing agents phalloidin (Tocris), colchicines and paclitaxel (Taxol; Sigma) were made up as concentrated stocks in water or dimethyl sulfoxide and stored at  $-20^\circ\text{C}$ . Stocks were thawed and diluted immediately before use. The amino acid sequence for the dynamin inhibitory peptide is QVPSRPNRP. The peptide derived from the GluR2 C terminus that binds to GRIP is YGIESVKIA. The peptide obtained from the GluR1 C terminus that interacts with synapse-associated protein 97 (SAP97) is SSGMPLGATGL. Antibodies were dialyzed into neurons through the patch electrode to perturb the function of endogenous proteins, including anti-kinesin (clone IBII; Sigma) and anti-SAP97 antibodies (Santa Cruz Biotechnology). Electrophysiological recordings were performed at least 20 min upon antibody infusion. Dialysis with peptides or antibodies through the patch pipette to influence intracellular proteins is a well established approach widely used in patch clamp recordings, which can be found in our previous publications (21, 24).

**Electrophysiological Recording in PFC Slices**—Pyramidal neurons located in layer V of PFC from Sprague-Dawley rats (3–4 weeks postnatal) were recorded. Slice preparation procedures were similar to what was described before (25, 26). In brief, animals were anesthetized by inhaling 2-bromo-2-chloro-1,1,1-trifluoroethane (1 ml/100 g; Sigma) and decapitated. Brains were quickly removed and sliced (300  $\mu\text{m}$ ) with a Leica VP1000S Vibrotome while bathed in a HEPES-buffered salt solution. Slices were then incubated for 1–5 h at room temperature (22–24  $^\circ\text{C}$ ) in a  $\text{NaHCO}_3$ -buffered saline (EBSS) bubbled with 95%  $\text{O}_2$ , 5%  $\text{CO}_2$ . Slices were pretreated with bicuculline (10  $\mu\text{M}$ ) or TTX (0.5  $\mu\text{M}$ ; both 2 h), similar to that in culture recordings. These reagents were washed off for  $\sim 0.5$  h before recordings, and care was taken to finish recordings within  $\sim 1.5$  h after treatments.

To measure AMPAR-mediated synaptic transmission, we performed the standard whole cell recording techniques in PFC slices (21, 26). Patch pipettes were filled with the same internal solution as that used in culture recordings. PFC slices were perfused with oxygenated artificial cerebrospinal fluid (130 mM NaCl, 26 mM  $\text{NaHCO}_3$ , 1 mM  $\text{CaCl}_2$ , 5 mM  $\text{MgCl}_2$ , 3 mM KCl, 10 mM glucose, 1.25 mM  $\text{NaH}_2\text{PO}_4$ ). Neurons were observed with a  $\times 40$  water-immersion lens and illuminated with near infrared light, and the image was captured with an infrared-sensitive CCD camera. Recordings were performed using a Multiclamp 700A amplifier (Axon Instruments). Tight seals (2–10 gOhms) were obtained by applying negative pressure. The membrane was disrupted with additional suction, and the whole cell configuration was obtained. Neurons were held at  $-70$  mV, which is close to the measured  $E_{\text{Cl}^-}$  ( $-69.8 \pm 0.1$  mV,  $n = 10$ ). Bipolar tungsten electrode (FHC, Inc.) was used to evoke EPSCs by stimulating the neighboring neurons (50- $\mu\text{s}$  pulse).

AMPA-EPSC was evoked every 10 s. Data analyses were performed with the Clampfit software (Axon Instruments).

**Transfection, Viral Infection, Small Interference RNA (siRNA), and Antisense**—Cultured PFC neurons (14–21 days *in vitro*) were transfected with  $D_4$  siRNA (Santa Cruz Biotechnology), CaMKII siRNA (Ambion), dominant negative KIF5 (dnKIF5), or SAP97 siRNA (Santa Cruz Biotechnology) using the Lipofectamine 2000 method (24, 25). EGFP (Clontech) was co-transfected. Recording was performed in GFP-positive neurons 2–3 days after transfection. To overexpress active CaMKII, we infected PFC cultures (14 days *in vitro*) with truncated CaMKII Sindbis virus (tCaMKII, 1–3  $\mu\text{l/ml}$  medium, a gift from Dr. Julius Zhu at the University of Virginia). The biochemical experiment was performed 1 day after virus exposure. To knock down the expression of MAP2 in cultured PFC neurons, we used the antisense oligonucleotide 5'-TCGTCAGC-CATCCTTCAGATCTCT-3' (27). The MAP2 sense oligonucleotide was used as a control. On DIV14, 1  $\mu\text{M}$  of oligonucleotides were added directly to the culture medium. Two to 3 days after being exposed to these oligonucleotides, biochemical assays were performed on the cultured neurons.

**Microtubule Stability Assay**—Free tubulin was extracted as described previously (25). After pretreatment of bicuculline (10  $\mu\text{M}$ , 2 h), virus infection or antisense application, cultured PFC neurons (14 days *in vitro*) in 3.5-cm dishes were washed twice with 1 ml of microtubule-stabilizing buffer (0.1 M MES, pH 6.75, 1 mM  $\text{MgSO}_4$ , 2 mM EGTA, 0.1 mM EDTA, and 4 M glycerol). Cells were then incubated at 37  $^\circ\text{C}$  for 5 min in 600  $\mu\text{l}$  of soluble tubulin extraction buffer (0.1 M MES, pH 6.75, 1 mM  $\text{MgSO}_4$ , 2 mM EGTA, 0.1 mM EDTA, 4 M glycerol, and 0.1% Triton X-100) with the addition of protease inhibitor mixture tablets (Roche Diagnostics). The soluble extract was centrifuged at 37  $^\circ\text{C}$  for 2 min, and the supernatant was saved. An equal amount of protein was separated by 7.5% SDS-PAGE. Western blotting was performed using primary antibodies against  $\alpha$ -tubulin and actin (both 1:2000; Sigma). Quantitative analysis was performed using ImageJ software.

**Immunocytochemistry**—After co-transfection of siRNA and EGFP, PFC cultures (21–24 days *in vitro*), were fixed (4% paraformaldehyde, 20 min), permeabilized (0.2% Triton X-100, 10 min), and blocked (5% BSA, 1 h). Neurons were next incubated with the antibody from antibody- $D_4$ R (sc-136169, 1:500; Santa Cruz Biotechnology), SAP97 (sc-9961, 1:500; Santa Cruz Biotechnology), MAP2 (sc-80012, 1:500; Santa Cruz Biotechnology), or PSD-95 (MA1-046, 1:500; Affinity Bioreagents) at 4  $^\circ\text{C}$  overnight. After three washes, they were incubated with the Alexa Fluor 594- (red) or Alexa Fluor 488- (green) conjugated secondary antibody (1:200, Molecular Probes) at room temperature for 1 h. Following three washes, the coverslips were mounted on slides with VECTASHIELD mounting media (Vector Laboratories). Fluorescent images were captured with a  $40\times$  or  $100\times$  objective and a cooled CCD camera mounted on a Nikon microscope using identical parameters.

## RESULTS

**$D_4$ R Bi-directionally Regulates AMPAR Synaptic Response in an Activity-dependent Manner**—To investigate whether  $D_4$  regulates AMPARs in an activity-dependent manner, we

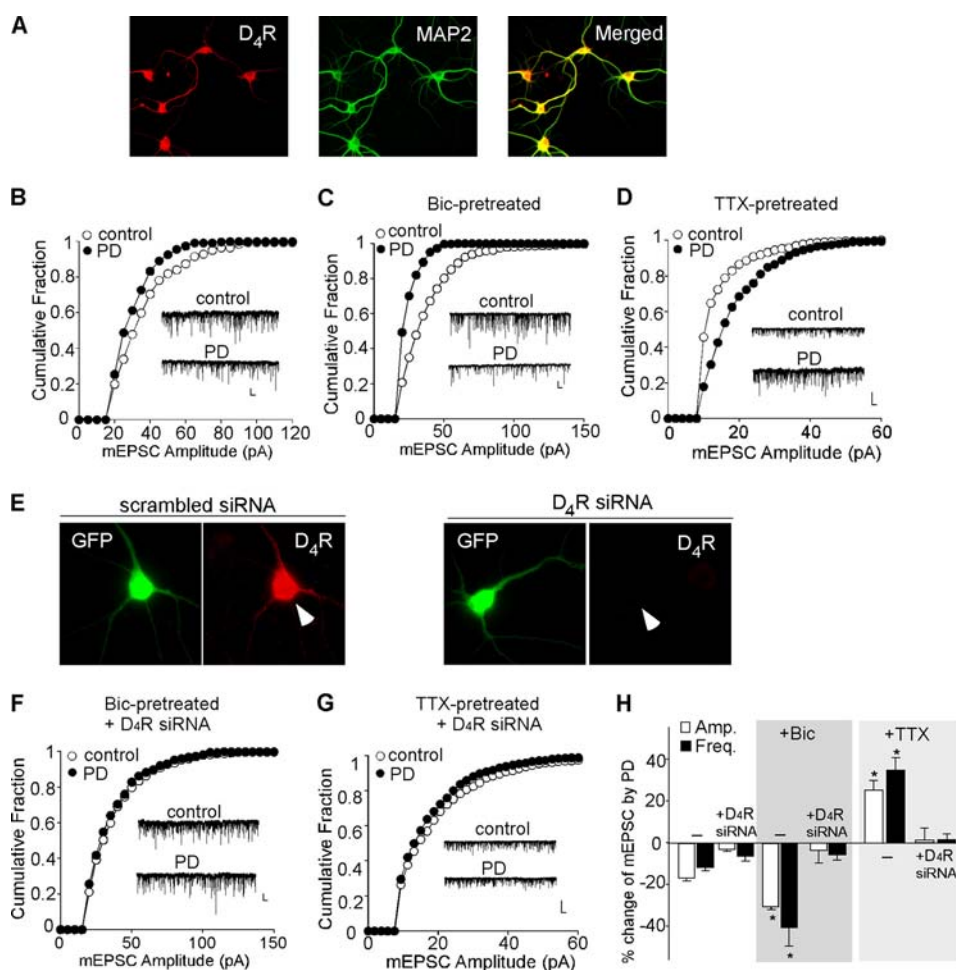


**FIGURE 1.  $D_4$  exerts an activity-dependent bi-directional regulation of spontaneous AMPAR synaptic responses in cultured PFC pyramidal neurons.** *A*, immunocytochemical images showing the co-expression of  $D_4R$  (red) and MAP2 (green) in cultured PFC neurons. *B–D*, cumulative plot of the distribution of mEPSC amplitudes before (control) and after PD168077 application in bicuculline (Bic; 10  $\mu$ M, 2 h)- or TTX (0.5  $\mu$ M, 2 h)-pretreated PFC cultures. *Insets*, representative mEPSC traces. *Scale bars*, 25 pA, 1 s. *E*, immunostaining of  $D_4R$  (red) in representative GFP-positive neurons transfected with a scrambled siRNA (left) or with a  $D_4R$  siRNA (right). *Arrowheads* point to GFP<sup>+</sup> neurons. *F* and *G*, cumulative plots of the distribution of mEPSC amplitudes before (control) and after PD168077 application in bicuculline- or TTX-pretreated PFC cultures transfected with a  $D_4R$  siRNA. *Scale bars*, 25 pA, 1 s. *H*, bar graphs (mean  $\pm$  S.E. (error bars)) showing the percentage change of mEPSC amplitude and frequency by PD168077 in different conditions. \*,  $p < 0.001$ , ANOVA.

recorded mEPSC, which represents the postsynaptic response to release of individual vesicles of glutamate, in cultured PFC pyramidal neurons pretreated with bicuculline (10  $\mu$ M, 2 h) or TTX (0.5  $\mu$ M, 2 h). Application of (2,3-dihydroxy-6-nitro-7-sulfamoyl-benzof[quinoxaline-2,3-dione (NBQX, 10  $\mu$ M) completely eliminated the mEPSC ( $n = 6$ ), indicating that it is mediated by AMPARs. Co-staining with the neuronal marker MAP2 (Fig. 1*A*) indicated that  $D_4R$  was present in almost all the cultured PFC neurons. Bath application of PD168077 (40  $\mu$ M, 10 min) caused a small reduction of the mEPSC amplitude (as indicated by a leftward shift of the distribution) in untreated cultures (Fig. 1*B*,  $16.8 \pm 1.2\%$ ,  $n = 11$ , Fig. 1*H*), although this reducing effect of PD168077 was significantly augmented in bicuculline-pretreated cultures (Fig. 1*C*,  $30.2 \pm 1.3\%$ ,  $n = 10$ , Fig. 1*H*). The mEPSC frequency was also decreased to a larger extent by PD168077 in cultures pretreated with bicuculline (untreated:  $11.1 \pm 1.5\%$ ,  $n = 11$ ; bicuculline-treated:  $40.1 \pm 8.9\%$ ,  $n = 10$ , Fig. 1*H*). However, in TTX-pretreated cultures, PD168077 significantly increased the mEPSC amplitude (Fig. 1*D*,  $25.1 \pm 4.7\%$ ,  $n = 12$ , Fig. 1*H*) and frequency ( $34.2 \pm 5.8\%$ ,  $n = 12$ , Fig. 1*H*).

To test whether this bi-directional effect of PD168077 is mediated by  $D_4$  receptors, we transfected PFC cultures with a  $D_4R$  siRNA. Specific knockdown of  $D_4R$  was validated by immunocytochemistry (Fig. 1*E*). Cellular knockdown of  $D_4R$  abolished the reducing effect of PD168077 on mEPSC in bicuculline-pretreated PFC cultures (Fig. 1*F*, amplitude:  $2.8 \pm 5.9\%$ ; frequency:  $5.6 \pm 2.5\%$ ;  $n = 8$ , Fig. 1*H*) and the enhancing effect of PD168077 on mEPSC in TTX-pretreated PFC cultures (Fig. 1*G*, amplitude:  $1.5 \pm 5.9\%$ ; frequency:  $1.3 \pm 2.6\%$ ;  $n = 7$ , Fig. 1*H*). Taken together, these results show that AMPAR-mediated synaptic response is suppressed by  $D_4$  at the high activity state and potentiated by  $D_4$  at the low activity state in cultured PFC neurons, consistent with the dual effects of  $D_4$  on evoked AMPAR-EPSC in PFC slices (21).

*Dual Regulation of AMPARs by  $D_4R$  Relies on CaMKII*—Next, we examined the involvement of CaMKII in the dual effects of  $D_4R$  in PFC cultures at different activity states. We first infected PFC cultures with the constitutively active CaMKII Sindbis virus (tCaMKII). As shown in Fig. 2*A*, in bicuculline-pretreated PFC cultures, the reducing effect of PD168077 on mEPSC was abolished in neurons infected with

## Mechanisms for $D_4$ Modulation of AMPARs

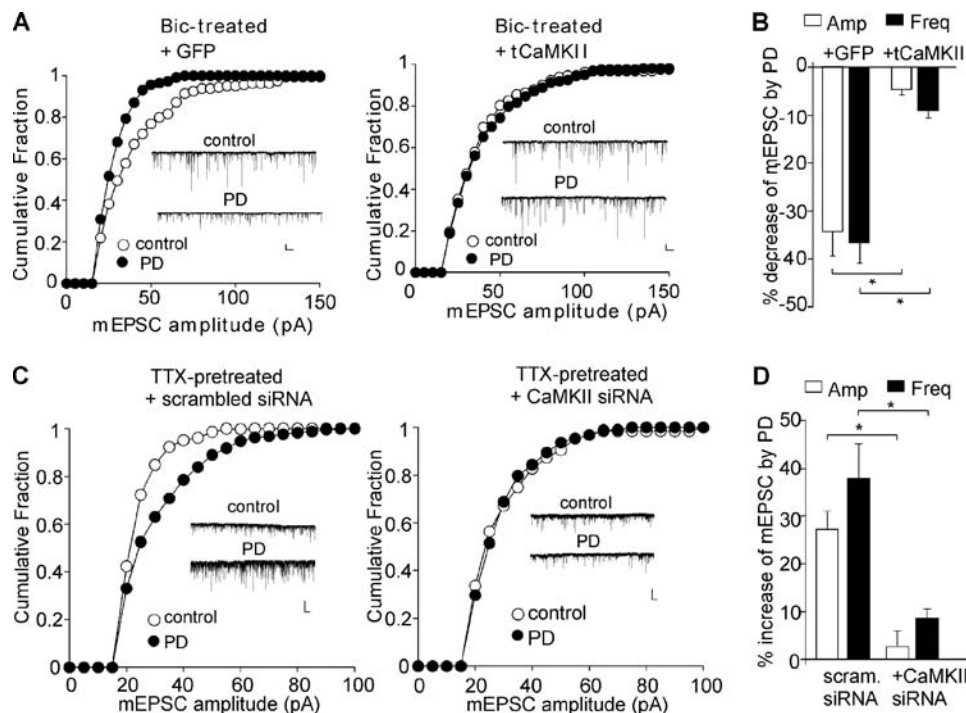


**FIGURE 2. CaMKII is involved in the bi-directional regulation of AMPAR currents by  $D_4$ R in PFC cultures.** A and C, cumulative plots of the distribution of mEPSC amplitude showing the effect of PD168077 in bicuculline (Bic;  $10 \mu\text{M}$ , 2 h)-pretreated PFC cultures infected with tCaMKII versus GFP Sindbis virus (A) or in TTX ( $0.5 \mu\text{M}$ , 2 h)-pretreated cultures transfected with CaMKII siRNA versus a scrambled siRNA (C). Insets, representative mEPSC traces. Scale bars, 20 pA, 1 s. \*,  $p < 0.001$ , ANOVA. B and D, bar graphs (mean  $\pm$  S.E. (error bars)) summarizing the percentage changes of mEPSC by PD168077 in different conditions.

tCaMKII (amplitude:  $4.7 \pm 1.1\%$ ; frequency:  $9.0 \pm 1.6\%$ ,  $n = 6$ , Fig. 2B), but not those infected with GFP Sindbis virus (amplitude:  $34.2 \pm 4.9\%$ ; frequency:  $36.4 \pm 4.2\%$ ,  $n = 5$ , Fig. 2B).

To test the role of CaMKII further, we transfected cultured PFC neurons with a CaMKII siRNA. Our previous studies have shown that this CaMKII siRNA causes an effective knockdown of CaMKII expression (24). As shown in Fig. 2C, in TTX-pretreated PFC cultures, the enhancing effect of PD168077 on mEPSC was lost in CaMKII siRNA-transfected neurons (amplitude:  $2.3 \pm 3.1\%$ ; frequency:  $8.3 \pm 1.9\%$ ,  $n = 6$ , Fig. 2D), but not those transfected with a scrambled siRNA (amplitude:  $27.5 \pm 3.6\%$ ; frequency:  $38.0 \pm 7.2\%$ ,  $n = 6$ , Fig. 2D). Taken together, these results suggest that CaMKII plays a key role the homeostatic regulation of AMPARs by  $D_4$  receptors in cultured PFC neurons.

**$D_4$  Depression of AMPARs at the High Activity State Is through a Mechanism Involving Microtubule/Kinesin Motor-based Transport of AMPARs**—To examine the possible mechanism by which  $D_4$  reduces AMPAR trafficking and function at the high activity state, we first tested the involvement of cytoskeletons. As shown in Fig. 3A, dialysis with paclitaxel ( $10 \mu\text{M}$ ), a microtubule stabilizer, caused little change on AMPAR-EPSC by itself ( $7.8 \pm 2.8\%$ ,  $n = 5$ ) but blocked the reducing effect of PD168077 ( $4.1 \pm 1.7\%$ ,  $n = 6$ , Fig. 3D). Bath application of the microtubule destabilizer colchicine ( $30 \mu\text{M}$ ) reduced basal AMPAR-EPSC and occluded the effect of PD168077 ( $8.2 \pm 2.0\%$ ,  $n = 7$ , Fig. 3D). However, the actin stabilizer phalloidin ( $10 \mu\text{M}$ ) did not alter the effect of PD168077 ( $40.1 \pm 2.4\%$ ,  $n = 4$ , Fig. 3D). Furthermore, dialysis with dynamin inhibitory peptide ( $100 \mu\text{M}$ ) failed to block the effect of PD168077 ( $47.5 \pm 1.5\%$ ,  $n = 8$ , Fig. 3D). These results suggest the involvement of

microtubules, but not actin or clathrin/dynamin-dependent endocytosis, in the  $D_4$  regulation of AMPARs.

Biochemical evidence shows that AMPAR and its binding protein GRIP are transported on microtubules by the kinesin motor protein KIF5 (28). To test further whether  $D_4$  activation might suppress AMPAR synaptic delivery by interfering with the MT/KIF5/GRIP-mediated transport of AMPA receptors, we tested the role of GRIP in  $D_4$  regulation of AMPAR-EPSC. A peptide derived from the C-terminal of GluR2 subunits (amino acids 871–883), which contains a functional sequence YGIES-VKIA that interferes with the endogenous GluR2-GRIP binding (29), was applied through the recording pipette. As shown in Fig. 3B, dialysis of the GluR2CT peptide ( $100 \mu\text{M}$ ) reduced AMPAR-EPSC ( $51.2 \pm 3.8\%$ ,  $n = 6$ ) and occluded the effect of PD168077 ( $5.4 \pm 1.6\%$ ,  $n = 5$ , Fig. 3D). A scrambled control peptide ( $100 \mu\text{M}$ ) failed to change AMPAR-EPSC or the reducing effect of PD168077 ( $49.4 \pm 2.1\%$ ,  $n = 5$ , Fig. 3D).

To examine the involvement of kinesin motors directly, we dialyzed a monoclonal antibody against KIF5, which is known to bind to kinesin and block the motor function (30), and examined the effect of PD168077 on AMPAR-EPSC in bicuculline-pretreated slices. As shown in Fig. 3C, dialyzing internal solution with anti-KIF5 ( $17 \mu\text{g/ml}$ ) caused a gradual decline of AMPAR-EPSC ( $51.7 \pm 6.3\%$ ,  $n = 6$ ), consistent with the previous report (31), and markedly attenuated the reduction of AMPAR-EPSC by PD168077 ( $3.6 \pm 1.6\%$ ,  $n = 8$ , Fig. 3D). Injection of the heat-inactivated anti-KIF5 failed to alter AMPAR-EPSC or the PD168077-mediated reduction of AMPAR-EPSC ( $43.8 \pm 3.9\%$ ,  $n = 4$ , Fig. 3D). In contrast, dialysis with anti-KIF5 did not alter the enhancing effect of PD168077 on AMPAR-

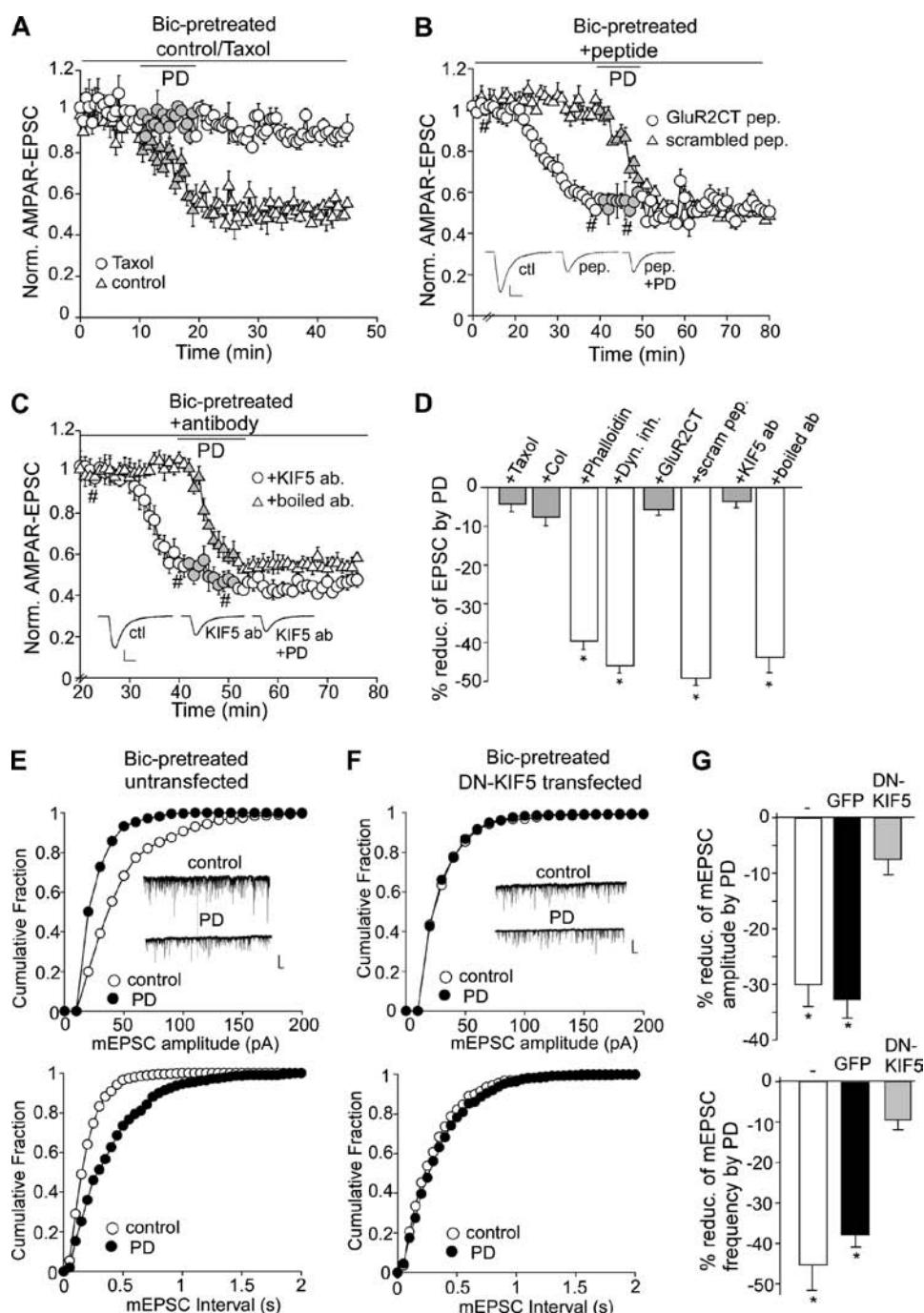


**FIGURE 3.  $D_4$ -induced synaptic depression in high activity PFC pyramidal neurons involves KIF5-mediated transport of the AMPAR-GRIP complex along microtubules.** A–C, plots of AMPAR-EPSC showing the effect of PD168077 in neurons (bicuculline (*Bic*)-pretreated) injected with the microtubule stabilizer paclitaxel (*Taxol*;  $10 \mu\text{M}$ , A), the GluR2 C-terminal peptide versus a scrambled control peptide ( $100 \mu\text{M}$ , B), or the antibody against KIF5 versus the boiled control antibody ( $17 \mu\text{g/ml}$ , C). Each point is the average of three or six traces. *Insets*, representative current traces at time points denoted by #. *Scale bars*, 50 pA, 10 ms. *D*, bar graphs (mean  $\pm$  S.E. (*error bars*)) showing the percentage reduction of AMPAR-EPSC by PD168077 in the presence of various agents. \*,  $p < 0.001$ , ANOVA. *E* and *F*, cumulative plots of the distribution of mEPSC amplitudes (*upper panels*) and mEPSC intervals (*lower panels*) before (*control*) and after PD168077 application in cultured PFC pyramidal neurons untransfected (*E*) or transfected with the dominant negative (DN) KIF5 (*F*). After transfection, cultures were pretreated with bicuculline ( $10 \mu\text{M}$ , 2 h) before recording. *Insets*, representative mEPSC traces. *Scale bars*, 25 pA, 1 s. *G*, bar graphs (mean  $\pm$  S.E.) showing the percentage reduction of mEPSC amplitude (*upper panel*) and frequency (*lower panel*) by PD168077 in PFC pyramidal neurons either untransfected or transfected with GFP or dominant negative KIF5. \*,  $p < 0.001$ , ANOVA.

EPSC in TTX-pretreated neurons ( $55.0 \pm 3.2\%$ ,  $n = 8$ ; [supplemental Fig. 1A](#)).

To examine further the involvement of KIF5 motor proteins in the  $D_4$  action, we transfected PFC cultures with a dominant negative KIF5 construct (generated by deleting the motor

domain) and examined the effect of PD168077 on mEPSC in transfected neurons. As shown in Fig. 3, *E–G*, in untransfected neurons (bicuculline-pretreated for 2 h), PD168077 caused a potent reduction of mEPSC amplitude ( $30.8 \pm 3.6\%$ ,  $n = 13$ ) and frequency ( $46.7 \pm 6.9\%$ ,  $n = 13$ ). Similar reduction was

## Mechanisms for $D_4$ Modulation of AMPARs

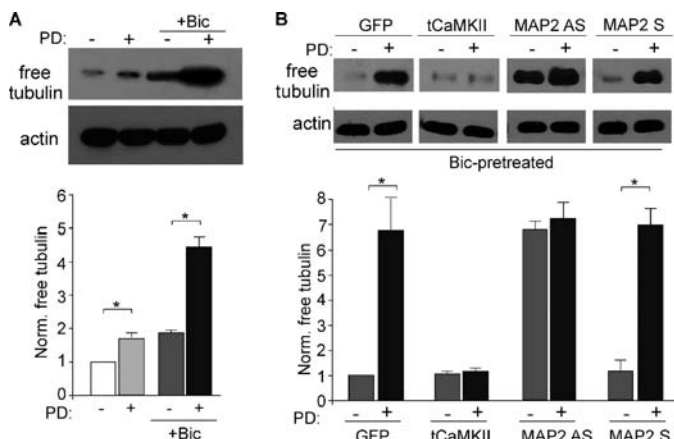


**FIGURE 4.  $D_4$  reduces microtubule stability in high activity PFC pyramidal neurons via a mechanism dependent on CaMKII and MAP2.** A, immunoblots and quantification of free tubulin showing the effect of PD168077 treatment ( $40 \mu\text{M}$ , 10 min) on microtubule depolymerization in PFC cultures pretreated without or with bicuculline (Bic;  $10 \mu\text{M}$ , 2 h). \*,  $p < 0.001$ , ANOVA. B, immunoblots and quantification of free tubulin showing the effect of PD168077 on microtubule depolymerization in PFC cultures (bicuculline-pretreated) infected with GFP versus constitutively active CaMKII Sindbis virus, or treated with MAP2 antisense versus sense oligonucleotides ( $1 \mu\text{M}$ ). Free tubulin was normalized to GFP-infected neurons in the absence of PD168077. \*,  $p < 0.001$ , ANOVA.

found in GFP-transfected neurons (amplitude:  $32.6 \pm 3.3\%$ ; frequency:  $37.4 \pm 3.1\%$ ,  $n = 7$ ). However, in dominant negative KIF5-transfected neurons (bicuculline-pretreated), the basal mEPSC amplitude was significantly smaller (untransfected:  $41.6 \pm 1.3 \text{ pA}$ ,  $n = 13$ ; transfected:  $24.4 \pm 1.4 \text{ pA}$ ,  $n = 14$ ;  $p < 0.001$ , ANOVA), whereas mEPSC frequency was largely unchanged (untransfected:  $4.3 \pm 0.5 \text{ Hz}$ ,  $n = 13$ ; transfected:  $4.6 \pm 0.5 \text{ Hz}$ ,  $n = 14$ ). Moreover, application of PD168077 had significantly diminished the effect on mEPSC amplitude ( $7.3 \pm 1.7\%$ ,  $n = 14$ ) and frequency ( $9.1 \pm 2.0\%$ ,  $n = 14$ ). It suggests that dominant negative KIF5 impairs the transport of functional AMPARs and occludes the reducing effect of  $D_4$  receptors. Taken together, these data provide multiple lines of evidence demonstrating that  $D_4$ -induced depression of AMPAR-EPSC involves the KIF5-mediated transport of AMPAR-GRIP complex along microtubules on dendrites.

**CaMKII Is Involved in  $D_4$  Depression of Microtubule-based AMPAR Trafficking at the High Activity State**—Because  $D_4$ -induced depression of glutamatergic transmission depends on the regulation of microtubule stability, we would like to know what molecules link  $D_4$  receptors to the microtubule network. One possible mechanism to change microtubule dynamics is to change the phosphorylation state of MAP2, a dendrite-specific microtubule-associated protein (32), therefore altering the association of MAP2 with microtubules and microtubule stability (33, 34). CaMKII, which is primarily expressed in glutamatergic neurons, is known to phosphorylate MAP2 in the microtubule binding domain (35). Thus, we performed biochemical assays to test whether  $D_4$  activation alters microtubule stability via a mechanism dependent on CaMKII and MAP2.

Western blot analysis was conducted in PFC cultures to detect the level of free tubulin (25), an indicator of microtubule depolymerization. As shown in Fig. 4A, application of PD168077 ( $40 \mu\text{M}$ , 10 min) caused a small increase in free tubu-

lin ( $1.67 \pm 0.14$ -fold of control,  $n = 3$ ), and this increase was more prominent in bicuculline ( $10 \mu\text{M}$ , 2 h)-pretreated neurons (bicuculline:  $1.86 \pm 0.06$ -fold of control; bicuculline + PD:  $4.46 \pm 0.28$ -fold of control,  $n = 3$ ), suggesting that the  $D_4$  reduction of microtubule stability is activity-dependent.

To test the role of CaMKII in  $D_4$  regulation of MT stability, we infected PFC cultures with constitutively active CaMKII Sindbis virus (tCaMKII). Cultures were treated with bicuculline for 2 h at 1 day after viral infection, followed by PD168077 application ( $40 \mu\text{M}$ , 10 min). As shown in Fig. 4B,  $D_4$  activation significantly increased free tubulin in GFP-infected neurons ( $6.7 \pm 1.3$ -fold of control,  $n = 5$ ), but failed to do so in tCaMKII-infected cultures ( $1.2 \pm 0.1$ -fold of control,  $n = 5$ ). This suggests that  $D_4$  reduces MT stability at the high activity state by a mechanism depending on CaMKII inhibition.

To test the involvement of MAP2, we treated PFC cultures (14 days *in vitro*) with MAP2 antisense oligonucleotides (27) to inhibit the expression of MAP2. As shown in Fig. 4B, MAP2 antisense treatment caused a significant elevation of the level of free tubulin and occluded the enhancing effect of  $D_4$  (MAP2 antisense:  $6.8 \pm 0.33$ -fold of control; MAP2 antisense + PD:  $7.3 \pm 0.65$  of control,  $n = 3$ ), whereas MAP2 sense oligonucleotide was ineffective (MAP2 sense:  $1.2 \pm 0.42$ -fold of control; MAP2 sense + PD:  $7.0 \pm 0.7$  of control,  $n = 3$ ). This suggests that the  $D_4$  reduction of MT stability at a high activity state is through a mechanism involving MAP2.

**SAP97 Is Involved in the  $D_4$ /CaMKII Enhancement of AMPAR Synaptic Delivery and Synaptic Transmission at the Low Activity State**—Next, we examined the potential mechanism involved in  $D_4$ /CaMKII-mediated increase of AMPAR trafficking and function in low activity PFC neurons. Previous studies have shown that SAP97, a member of membrane-associated guanylate kinase protein family, is selectively associated with GluR1 subunit (36, 37), and CaMKII-dependent phosphorylation of SAP97 at Ser<sup>39</sup> leads to increased targeting of SAP97 into dendritic spines (38). Thus, SAP97 provides a possible link between  $D_4$ -activated CaMKII and increased AMPAR surface delivery in PFC pyramidal neurons at the low activity state. To test this, we transfected PFC cultures with a SAP97 siRNA (GFP co-transfected). As shown in Fig. 5A, this SAP97 siRNA specifically knocked down the expression of SAP97 (in GFP<sup>+</sup> neurons), but not the homolog protein PSD-95. After transfection, neurons were pretreated with TTX ( $0.5 \mu\text{M}$ , 2 h) before recording. As shown in Fig. 5, B and C, in neurons transfected with a scrambled siRNA, PD168077 significantly increased mEPSC (amplitude:  $29.8 \pm 3.2\%$ ,  $n = 8$ ; frequency:  $41.1 \pm 7.2\%$ ,  $n = 9$ ). Transfection of SAP97 siRNA caused a slight reduction of basal mEPSC amplitude (scrambled siRNA:  $26.1 \pm 1.7 \text{ pA}$ ,  $n = 9$ ; SAP97 siRNA:  $20.1 \pm 1.9 \text{ pA}$ ,  $n = 7$ ;  $p < 0.05$ , ANOVA), but not frequency (scrambled siRNA:  $3 \pm 0.64 \text{ Hz}$ ,  $n = 9$ ; SAP97 siRNA:  $2.7 \pm 0.47 \text{ Hz}$ ,  $n = 7$ ). Moreover, the enhancing effect of PD168077 on mEPSC was significantly diminished in neurons transfected with SAP97 siRNA (amplitude:  $8 \pm 3.0\%$ ,  $n = 7$ ; frequency:  $10.7 \pm 4.1\%$ ,  $n = 7$ ).

To examine the role of SAP97 further, we dialyzed neurons with a peptide derived from the GluR1 C-terminal region containing the SSG sequence that is essential for the binding to SAP97 (37). As shown in Fig. 5D, loading the SSG peptide (50

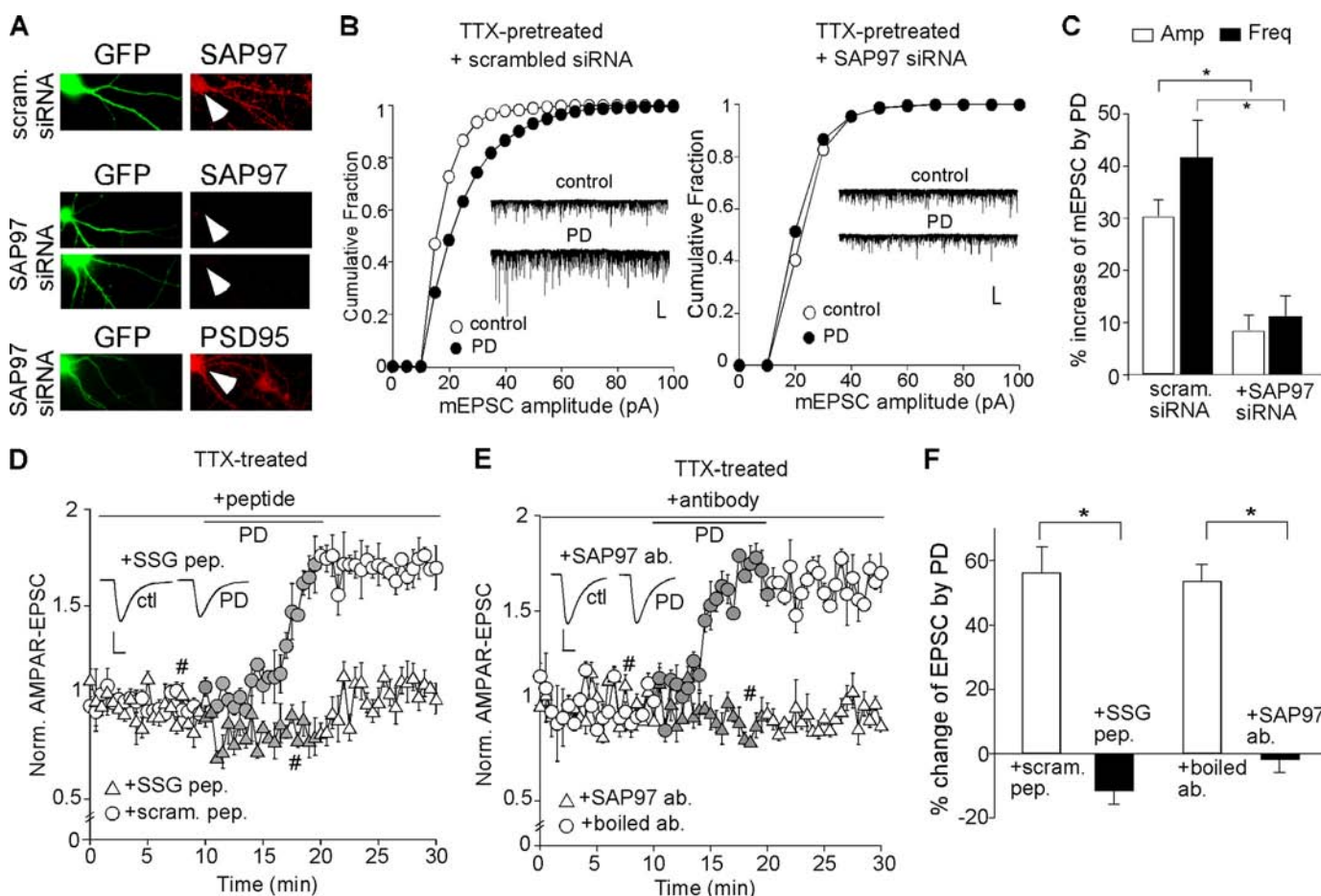


**FIGURE 5. SAP97 is involved in  $D_4$  potentiation of AMPAR transmission in PFC pyramidal neurons at the low activity state.** *A*, immunocytochemical staining of SAP97 or PSD95 (red) in cultured (14–16 or 21–24 days *in vitro*) PFC neurons transfected with SAP97 siRNA or a scrambled siRNA (co-transfected with GFP). Arrowheads point to GFP<sup>+</sup> neurons. *B*, cumulative plots of the distribution of mEPSC amplitudes before (control) and after PD168077 application in scrambled siRNA-transfected or SAP97 siRNA-transfected PFC pyramidal neurons pretreated with TTX (0.5  $\mu$ M, 2 h). Insets, representative mEPSC traces. Scale bars, 20 pA, 1 s. *C*, bar graphs (mean  $\pm$  S.E. (error bars)) showing the percentage increase of mEPSC amplitude and frequency by PD168077 in TTX-pretreated PFC pyramidal neurons transfected with a scrambled siRNA or SAP97 siRNA. \*,  $p < 0.001$ , ANOVA. *D* and *E*, plot of AMPAR-EPSC showing the effect of PD168077 in PFC pyramidal neurons (TTX-pretreated) injected with SSG peptide (50  $\mu$ M) versus a scrambled control peptide (*D*), or anti-SAP97 (10  $\mu$ g/ml) versus the heat-inactivated antibody (*E*). *F*, bar graphs (mean  $\pm$  S.E.) showing the percentage change of AMPAR-EPSC by PD168077 in the presence of various agents. \*,  $p < 0.001$ , ANOVA.

$\mu$ M) to disrupt GluR1/SAP97 interaction prevented the PD168077-induced increase of AMPAR-EPSC in TTX-pretreated PFC pyramidal neurons ( $-11.2 \pm 3.9\%$ ,  $n = 7$ , Fig. 5*F*), whereas a scrambled control peptide was ineffective ( $54.9 \pm 8.2\%$ ,  $n = 7$ , Fig. 5*F*). Dialysis of the SSG peptide alone did not induce significant changes in basal AMPAR-EPSC (data not shown).

Furthermore, we dialyzed neurons with an antibody against SAP97 (amino acids 1–229) to block the function of endogenous SAP97. As shown in Fig. 5*E*, the enhancing effect of PD168077 on AMPAR-EPSC was lost in PFC pyramidal neurons (TTX-pretreated) injected with anti-SAP97 (10  $\mu$ g/ml,  $-1.4 \pm 3.9\%$ ,  $n = 7$ , Fig. 5*F*), but not the heat-inactivated antibody ( $53.3 \pm 5.2\%$ ,  $n = 7$ , Fig. 5*F*). In contrast, dialysis with anti-SAP97 did not alter the reducing effect of PD168077 on AMPAR-EPSC in bicuculline-pretreated PFC pyramidal neurons ( $44.4 \pm 3.5\%$ ,  $n = 7$ ; supplemental Fig. 1*B*). These lines of evidence suggest that  $D_4$ -induced potentiation of AMPAR transmission in PFC pyramidal neurons at the low activity state is through a mechanism involving CaMKII/SAP97-mediated delivery of AMPARs to the synaptic membrane.

## DISCUSSION

Our recent studies have revealed the  $D_4$ -induced, CaMKII-dependent homeostatic regulation of AMPAR trafficking and function in PFC pyramidal neurons (21). In this study, we have revealed the mechanism downstream of CaMKII that underlies the unique action of  $D_4$  on AMPA receptors in PFC pyramidal neurons (Fig. 6). At the high activity state,  $D_4$  receptors depress AMPAR-EPSC via a mechanism involving decreased CaMKII activity and reduced transport of AMPAR subunits along dendritic microtubules. At the low activity state,  $D_4$  receptors potentiate AMPAR-EPSC via a mechanism depending on increased CaMKII activity and enhanced synaptic delivery of AMPA receptors via SAP97.

It is known that AMPAR trafficking plays a key role in controlling synaptic strength and plasticity. After being synthesized in the cell body, AMPARs are inserted into intracellular vesicles and move to dendrites where they become incorporated into synapses. Several mechanisms have been proposed to be important for regulating the localization of AMPARs at the synaptic membrane, including PDZ domain-mediated interac-

## Mechanisms for $D_4$ Modulation of AMPARs

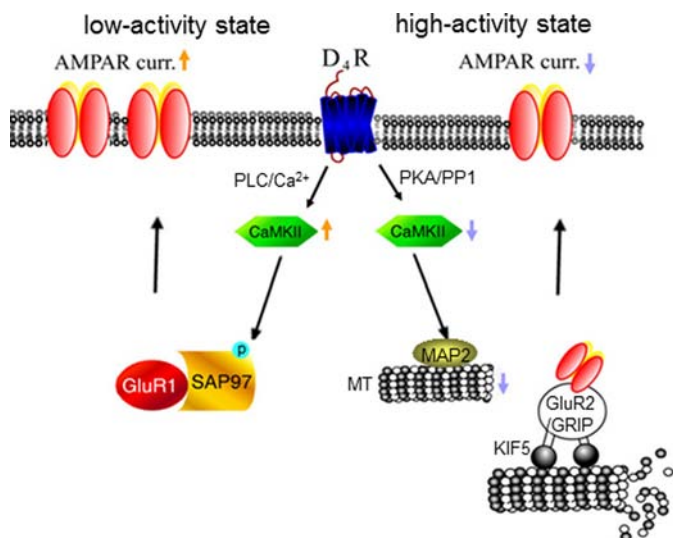


**FIGURE 6. Schematic diagram showing the homeostatic regulation of glutamatergic transmission by dopamine  $D_4$  receptors in PFC pyramidal neurons.** At the high activity state,  $D_4$  suppresses excitatory synaptic strength via a mechanism dependent on CaMKII-regulated microtubule/kinesin motor-based dendritic transport of AMPA receptors. At the low activity state,  $D_4$  potentiates excitatory synaptic strength via a mechanism involving CaMKII/SAP97-dependent synaptic delivery of AMPA receptors.

tions between channel subunits and synaptic scaffolding proteins (39, 40), clathrin/dynamin-dependent endocytosis (41, 42), and motor protein-based transport along microtubule or actin cytoskeletons (28, 43, 44). Biochemical studies have found that the AMPAR GluR2 subunit-interacting protein, GRIP, directly interacts and steers kinesin heavy chains to dendrites as a microtubule motor for AMPA receptors (28). In hippocampal neurons loaded with antibodies that inactivate the function of kinesin, AMPAR-EPSC is substantially reduced, suggesting that a labile pool of AMPARs is sensitive to microtubule motor inhibitors (31). In this study, we demonstrate that the  $D_4$ -induced depression of AMPAR-EPSC at the high activity state is not affected by manipulating endocytosis or actin cytoskeleton. Instead, it is prevented when MT stability is disturbed or the kinesin motor is suppressed or the GluR2/GRIP interaction is disrupted. This suggests that  $D_4$  suppresses AMPARs via a mechanism involving KIF5-mediated transport of GluR2-GRIP complex along microtubules on dendrites. Consistently, biochemical assays have shown that  $D_4$  activation induces a profound decrease of microtubule stability at high activity PFC neurons.

The potential molecule linking  $D_4$  receptors to the microtubule network is CaMKII, a kinase phosphorylating MAP2 in the microtubule binding domain (35) and therefore altering MAP2-microtubule association and microtubule stability (33, 34). Our previous studies have shown that at the high activity state,  $D_4$  stimulation decreases CaMKII activity via inhibition of PKA and disinhibition of protein phosphatase 1 (23), which causes the depression of AMPAR-EPSC (21). Here we have found that the  $D_4$ -induced microtubule depolymerization is blocked by constitutively active CaMKII or occluded by MAP2 suppression. This suggests that  $D_4$  inhibits MT stability by inhibiting CaMKII regulation of MAP2 at high activity PFC neurons.

On the other hand, the  $D_4$  potentiation of AMPAR-EPSC at the low activity state involves the  $D_4$  increase of CaMKII activity via the phospholipid pathway (23) and the CaMKII-induced synaptic delivery of AMPARs (21). How does activated CaMKII recruit AMPARs to synapses? Detailed mechanisms remain elusive. There is evidence showing that it requires the GluR1 and PDZ domain interaction (39). The GluR1 C terminus specifically binds to the PDZ domain-containing protein SAP97 (36, 37). Overexpression of SAP97 leads to an increase in synaptic AMPA receptors, spine enlargement, and an increase in mEPSC frequency (45). Moreover, overexpression of SAP97 during development traffics AMPARs to synapses (46), suggesting that SAP97 is part of the machinery that controls AMPAR trafficking. Genetic deletion of SAP97 does not alter synaptic transmission, which may be due to the compensation of other PSD-membrane-associated guanylate kinases (46). Consistently, we have found that knockdown of SAP97 with siRNA or disruption of GluR1/SAP97 interaction with the SSG peptide has little effect on basal mEPSC amplitude or frequency. However, the  $D_4$ /CaMKII-induced enhancement of mEPSC in TTX-pretreated neurons is blocked by SAP97 siRNA or SSG peptide, suggesting that SAP97 is involved in  $D_4$ /CaMKII-dependent delivery of AMPARs to synapses. At the low activity state,  $D_4$  stimulation increases CaMKII activity, which could trigger SAP97 phosphorylation at Ser<sup>39</sup>, causing increased targeting of SAP97 into dendritic spines (38). Consequently, GluR1, which binds to SAP97 (36, 37), is recruited to synapses. It awaits to be investigated how SAP97 is synaptic redistributed upon CaMKII phosphorylation.

Despite the variety of *in vitro* data indicating that AMPAR interactions with PDZ domain-containing proteins may be an important step for regulating the level of synaptic AMPARs during bi-directional plasticity, mice lacking the C-terminal PDZ ligand of GluR1 show no change in AMPAR trafficking, basal synaptic transmission, long-term potentiation or long-term depression (47). This suggests that the properties of AMPAR trafficking in cultures may be different from those *in vivo*. Whether SAP97 is required for the  $D_4$ -induced increase of synaptic GluR1 subunits in low activity cortical neurons *in vivo* awaits further investigation.

It is well recognized that dopaminergic inputs to the PFC are important for PFC-mediated cognitive functions including working memory (3–5). Because PFC excitatory transmission plays a key role in these cognitive processes (48), glutamate synapse components are the potential major targets of dopamine in PFC networks. PFC pyramidal cell excitability is enhanced or attenuated by the  $D_1$  or  $D_2$  receptor, respectively, via distinct mechanisms, depending on the glutamate receptor subtypes involved (49). Dopamine has been found to increase EPSC amplitude in layer II–III PFC pyramidal neurons via a  $D_1$ -mediated postsynaptic signaling cascade involving  $Ca^{2+}$ , PKA, and CaMKII (50). The dopamine-mediated reduction of excitatory neurotransmission in PFC pyramidal neurons has also been reported (51, 52). In PFC cultures,  $D_1$  facilitates AMPAR synaptic insertion via a PKA-dependent mechanism, whereas  $D_2$  decreases surface and synaptic GluR1 expression (53). Moreover, in ventral tegmental area-PFC co-cultures, dopamine agonists act on  $D_1$  receptors on PFC neurons, alter-



ing their excitatory transmission onto ventral tegmental area dopamine neurons, thus influencing AMPARs (54). In contrast to the positive or negative impact of D<sub>1</sub> or D<sub>2</sub> receptors on AMPAR trafficking and glutamatergic transmission in PFC neurons, our studies (21 and the present one) have shown that D<sub>4</sub> receptors exert a dynamic effect. At the high activity state, D<sub>4</sub> receptor, via CaMKII inhibition, reduces both GluR1 and GluR2 from synaptic membrane; at the low activity state, D<sub>4</sub> receptor, via CaMKII stimulation, promotes the delivery of GluR1 to synaptic membrane (21). This homeostatic regulation enables D<sub>4</sub> receptors to stabilize cortical excitability, which is consistent with the role of D<sub>4</sub> in ADHD (10, 11) and cortical hyperexcitability in D<sub>4</sub> knock-out mice (17).

*Acknowledgments*—We thank Xiaoqing Chen for excellent technical support and Jia Chen for help in some of the experiments.

## REFERENCES

- Wise, R. A. (2004) *Nat. Rev. Neurosci.* **5**, 483–494
- Kehagia, A. A., Murray, G. K., and Robbins, T. W. (2010) *Curr. Opin. Neurobiol.* **20**, 199–204
- Williams, G. V., and Goldman-Rakic, P. S. (1995) *Nature* **376**, 572–575
- Sawaguchi, T., and Goldman-Rakic, P. S. (1991) *Science* **251**, 947–950
- Wang, M., Vijayraghavan, S., and Goldman-Rakic, P. S. (2004) *Science* **303**, 853–856
- Mrzljak, L., Bergson, C., Pappy, M., Huff, R., Levenson, R., and Goldman-Rakic, P. S. (1996) *Nature* **381**, 245–248
- Wedzony, K., Chocyk, A., Maekowiak, M., Fijał, K., and Czyrak, A. (2000) *J. Physiol. Pharmacol.* **51**, 205–221
- Van Tol, H. H., Bunzow, J. R., Guan, H. C., Sunahara, R. K., Seeman, P., Niznik, H. B., and Civelli, O. (1991) *Nature* **350**, 610–614
- Kapur, S., and Remington, G. (2001) *Annu. Rev. Med.* **52**, 503–517
- LaHoste, G. J., Swanson, J. M., Wigal, S. B., Glabe, C., Wigal, T., King, N., and Kennedy, J. L. (1996) *Mol. Psychiatry* **1**, 121–124
- Van Tol, H. H., Wu, C. M., Guan, H. C., Ohara, K., Bunzow, J. R., Civelli, O., Kennedy, J., Seeman, P., Niznik, H. B., and Jovanovic, V. (1992) *Nature* **358**, 149–152
- Diaz-Anzaldúa, A., Joover, R., Rivière, J. B., Dion, Y., Lespérance, P., Richer, F., Chouinard, S., and Rouleau, G. A. (2004) *Mol. Psychiatry* **9**, 272–277
- Ray, L. A., Miranda, R., Jr., Tidey, J. W., McGeary, J. E., MacKillop, J., Gwaltney, C. J., Rohsenow, D. J., Swift, R. M., and Monti, P. M. (2010) *J. Abnorm. Psychol.* **119**, 115–125
- Ray, L. A., Bryan, A., MacKillop, J., McGeary, J., Hesterberg, K., and Hutchison, K. E. (2009) *Addict. Biol.* **14**, 238–244
- Durston, S., Fossella, J. A., Casey, B. J., Hulshoff Pol, H. E., Galvan, A., Schnack, H. G., Steenhuis, M. P., Minderaa, R. B., Buitelaar, J. K., Kahn, R. S., and van Engeland, H. (2005) *Mol. Psychiatry* **10**, 678–685
- Cheon, K. A., Kim, B. N., and Cho, S. C. (2007) *Neuropsychopharmacology* **32**, 1377–1383
- Rubinstein, M., Cepeda, C., Hurst, R. S., Flores-Hernandez, J., Ariano, M. A., Falzone, T. L., Kozell, L. B., Meshul, C. K., Bunzow, J. R., Low, M. J., Levine, M. S., and Grandy, D. K. (2001) *J. Neurosci.* **21**, 3756–3763
- Dulawa, S. C., Grandy, D. K., Low, M. J., Paulus, M. P., and Geyer, M. A. (1999) *J. Neurosci.* **19**, 9550–9556
- Rubinstein, M., Phillips, T. J., Bunzow, J. R., Falzone, T. L., Dziewczapolski, G., Zhang, G., Fang, Y., Larson, J. L., McDougall, J. A., Chester, J. A., Saez, C., Pugsley, T. A., Gershanik, O., Low, M. J., and Grandy, D. K. (1997) *Cell* **90**, 991–1001
- Zhang, K., Grady, C. J., Tsapakis, E. M., Andersen, S. L., Tarazi, F. I., and Baldessarini, R. J. (2004) *Neuropsychopharmacology* **29**, 1648–1655
- Yuen, E. Y., Zhong, P., and Yan, Z. (2010) *Proc. Natl. Acad. Sci. U.S.A.* **107**, 22308–22313
- Gu, Z., Jiang, Q., Yuen, E. Y., and Yan, Z. (2006) *Mol. Pharmacol.* **69**, 813–822
- Gu, Z., and Yan, Z. (2004) *Mol. Pharmacol.* **66**, 948–955
- Yuen, E. Y., Liu, W., Kafri, T., van Praag, H., and Yan, Z. (2010) *J. Physiol.* **588**, 2361–2371
- Yuen, E. Y., Jiang, Q., Feng, J., and Yan, Z. (2005) *J. Biol. Chem.* **280**, 29420–29427
- Yuen, E. Y., Liu, W., Karatsoreos, I. N., Feng, J., McEwen, B. S., and Yan, Z. (2009) *Proc. Natl. Acad. Sci. U.S.A.* **106**, 14075–14079
- Caceres, A., Mautino, J., and Kosik, K. S. (1992) *Neuron* **9**, 607–618
- Setou, M., Seog, D. H., Tanaka, Y., Kanai, Y., Takei, Y., Kawagishi, M., and Hirokawa, N. (2002) *Nature* **417**, 83–87
- Daw, M. I., Chittajallu, R., Bortolotto, Z. A., Dev, K. K., Duprat, F., Henley, J. M., Collingridge, G. L., and Isaac, J. T. (2000) *Neuron* **28**, 873–886
- Bananas, E., Murray, J. W., Stockert, R. J., Satir, P., and Wolkoff, A. W. (2000) *J. Cell Biol.* **151**, 179–186
- Kim, C. H., and Lisman, J. E. (2001) *J. Neurosci.* **21**, 4188–4194
- Caceres, A., Binder, L. I., Payne, M. R., Bender, P., Rebhun, L., and Steward, O. (1984) *J. Neurosci.* **4**, 394–410
- Brugg, B., and Matus, A. (1991) *J. Cell Biol.* **114**, 735–743
- Sánchez, C., Díaz-Nido, J., and Avila, J. (2000) *Prog. Neurobiol.* **61**, 133–168
- Schulman, H. (1984) *J. Cell Biol.* **99**, 11–19
- Leonard, A. S., Davare, M. A., Horne, M. C., Garner, C. C., and Hell, J. W. (1998) *J. Biol. Chem.* **273**, 19518–19524
- Cai, C., Coleman, S. K., Niemi, K., and Keinänen, K. (2002) *J. Biol. Chem.* **277**, 31484–31490
- Mauceri, D., Cattabeni, F., Di Luca, M., and Gardoni, F. (2004) *J. Biol. Chem.* **279**, 23813–23821
- Hayashi, Y., Shi, S. H., Esteban, J. A., Piccini, A., Poncer, J. C., and Malinow, R. (2000) *Science* **287**, 2262–2267
- Elias, G. M., Funke, L., Stein, V., Grant, S. G., Bredt, D. S., and Nicoll, R. A. (2006) *Neuron* **52**, 307–320
- Carroll, R. C., Beattie, E. C., Xia, H., Lüscher, C., Altschuler, Y., Nicoll, R. A., Malenka, R. C., and von Zastrow, M. (1999) *Proc. Natl. Acad. Sci. U.S.A.* **96**, 14112–14117
- Man, H. Y., Lin, J. W., Ju, W. H., Ahmadian, G., Liu, L., Becker, L. E., Sheng, M., and Wang, Y. T. (2000) *Neuron* **25**, 649–662
- Zhou, Q., Xiao, M., and Nicoll, R. A. (2001) *Proc. Natl. Acad. Sci. U.S.A.* **98**, 1261–1266
- Correia, S. S., Bassani, S., Brown, T. C., Lisé, M. F., Backos, D. S., El-Husseini, A., Passafaro, M., and Esteban, J. A. (2008) *Nat. Neurosci.* **11**, 457–466
- Rumbaugh, G., Sia, G. M., Garner, C. C., and Huganir, R. L. (2003) *J. Neurosci.* **23**, 4567–4576
- Howard, M. A., Elias, G. M., Elias, L. A., Swat, W., and Nicoll, R. A. (2010) *Proc. Natl. Acad. Sci. U.S.A.* **107**, 3805–3810
- Kim, C. H., Takamiya, K., Petralia, R. S., Sattler, R., Yu, S., Zhou, W., Kalb, R., Wenthold, R., and Huganir, R. (2005) *Nat. Neurosci.* **8**, 985–987
- Goldman-Rakic, P. S. (1995) *Neuron* **14**, 477–485
- Tseng, K. Y., and O'Donnell, P. (2004) *J. Neurosci.* **24**, 5131–5139
- Gonzalez-Islas, C., and Hablitz, J. J. (2003) *J. Neurosci.* **23**, 867–875
- Gao, W. J., Krimer, L. S., and Goldman-Rakic, P. S. (2001) *Proc. Natl. Acad. Sci. U.S.A.* **98**, 295–300
- Otani, S., Blond, O., Desce, J. M., and Crépel, F. (1998) *Neuroscience* **85**, 669–676
- Sun, X., Zhao, Y., and Wolf, M. E. (2005) *J. Neurosci.* **25**, 7342–7351
- Gao, C., and Wolf, M. E. (2007) *J. Neurosci.* **27**, 14275–14285